Accuracy Prediction of Higher-Order Structural Theories for 1D Aerospace Structures Using Neural Networks

Original
Accuracy Prediction of Higher-Order Structural Theories for 1D Aerospace Structures Using Neural Networks / Petrolo, M., Pagani, A., Carrera, E., Candita, G.. - ELETTRONICO. - 69:(2026), pp. 1176-1180. (10th CEAS Aerospace Europe Conference and 28th AIDAA International Congress Torino 1-4 December 2025) [10.21741/9781644904251-202].

Availability:
This version is available at: 11583/3013146 since: 2026-07-15T14:22:25Z

Publisher:
Materials Research Forum LLC

Published
DOI:10.21741/9781644904251-202

Materials Research Proceedings 69 (2026) 1176-1180 https://doi.org/10.21741/9781644904251-202

Accuracy Prediction of Higher-Order Structural Theories for 1D Aerospace Structures Using Neural Networks

Marco Petrolo[1,a] *, Alfonso Pagani[1,b], Erasmo Carrera[1,c], and Giulio Candita[1,d]

[1]MUL2 Lab, Department of Mechanical and Aerospace Engineering, Corso Duca degli Abruzzi 24, 10129, Torino, Italy

[a]marco.petrolo@polito.it, [b]alfonso.pagani@polito.it, [c]erasmo.carrera@polito.it, [d]giulio.candita@polito.it

Keywords: Aerospace Structures, CUF, Higher-Order Theories, Neural Networks

Abstract. This study introduces a Machine Learning (ML) framework to assess the accuracy of higher-order structural theories for aerospace structures. Stiffened panels are modeled using one-dimensional elements and analyzed using refined theories based on the Carrera Unified Formulation (CUF). To evaluate accuracy, the framework compares the average error of the first ten natural frequencies with that of a reference model. An ML tool automatically predicts this error and identifies the most relevant generalized variables for each structural configuration. The dataset used to train the ML tool is generated using CUF and includes material properties, geometry, and the structural theory generalized variables. To process this information, two types of Neural Networks (NN) are employed: a Convolutional Neural Network (CNN) extracts geometric features from cross-section images, e.g., number and position of stiffeners, and a Deep Neural Network (DNN) combines these features with material and geometric data to predict the accuracy of each theory. As a result, the framework effectively predicts the most accurate and computationally efficient theories and their associated generalized variables.

Introduction

In structural mechanics, creating accurate reduced models is crucial to lowering the computational complexity of 3D analyses. Since they have fewer degrees of freedom than 3D models, 1D and 2D theories are frequently employed. However, depending on the specific problem, the accuracy of these theories can vary significantly. Classical theories such as the Euler–Bernoulli Beam Theory (EBBT) [1] and the Timoshenko Beam Theory (TBT) [2,3] are often unable to capture complex behaviors such as material anisotropy, shear deformability, or warping effects. To overcome these limitations, higher-order theories (HOT) [4,5] have been developed to address more complex structural problems, including composites [6] and thick beams [7, 8]. The Carrera Unified Formulation (CUF) [9] provides a general and systematic framework for defining structural theories of any order. The Axiomatic/Asymptotic Method (AAM) [10] can be applied to determine the most influential unknowns in higher-order theories, enabling the selection of the most efficient theory for a given problem. However, AAM requires multiple evaluations of generalized variables, leading to high computational costs. In recent years, Machine Learning (ML) techniques [11] have attracted increasing attention in structural mechanics and finite element analysis due to their predictive capabilities and reduced computational time. Their applications include stress prediction, structural health monitoring, and topology optimization. The present paper combines a fully connected Deep Neural Network (DNN) and a Convolutional Neural Network (CNN) to reduce the computational cost of AAM and improve the accuracy of error prediction. The proposed framework extends the authors' previous works [12,13] to stiffened structures for aerospace applications.

CUF and FEM Formulations

The reference system adopted for beam structures is shown in Fig. 1. Here, the x-z plane lies on the cross-section Ω.

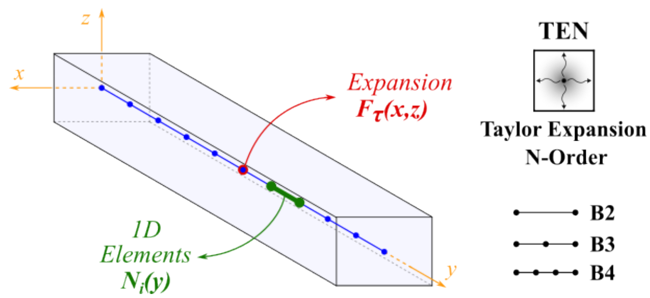

Figure 1: Reference coordinate system for beam models

The displacement field for beams can be expressed as:

$$\boldsymbol{u}(x,y,z) = N_i F_\tau(x,z)\boldsymbol{u}_{\tau i} \tag{1}$$

Where F_τ is the expansion function; τ=1,…, M, and M is the number of expansion terms. N_i is the shape function; $i = 1, \dots, N_n$, where N_n is the number of FE nodes. $\boldsymbol{u}_{\tau i}$ is the vector of the nodal unknowns. For 1D theories, the expansion function F_τ acts on the cross-section x-z, while the shape function along the beam axis. For a second-order beam theory, the displacement field is:

$$\begin{aligned} u_x &= u_{x_1} + xu_{x_2} + zu_{x_3} + x^2u_{x_4} + xzu_{x_5} + z^2u_{x_6} \\ u_y &= u_{y_1} + xu_{y_2} + zu_{y_3} + x^2u_{y_4} + xzu_{y_5} + z^2u_{y_6} \\ u_z &= u_{z_1} + xu_{z_2} + zu_{z_3} + x^2u_{z_4} + xzu_{z_5} + z^2u_{z_6} \end{aligned} \tag{2}$$

With a total of eighteen nodal displacement variables. The Principle of Virtual Displacements is used to derive the governing equations for the free vibration problem,

$$\delta L_{int} = \delta L_{ext} - \delta L_{ine} \tag{3}$$

The work done by internal forces is δL_{int}, by external forces is δL_{ext}, and by inertial forces is δL_{ine}. In this free-vibration case, the governing equation is the following:

$$\delta \boldsymbol{u}_{sj}: \quad \boldsymbol{m}_{\tau sij}\ddot{\boldsymbol{u}}_{\tau i} + \boldsymbol{k}_{\tau sij}\boldsymbol{u}_{\tau i} = 0 \tag{4}$$

$\boldsymbol{k}_{\tau sji}$ and $\boldsymbol{m}_{\tau sji}$ are the 3x3 Fundamental Nuclei (FN), for the stiffness and mass matrix, respectively. By solving the eigenvalue problem, natural frequencies, ω_n, and modal shapes are obtained:

$$(\boldsymbol{K} - \omega_n^2\boldsymbol{M})\boldsymbol{U} = 0 \tag{5}$$

Neural Networks

The Neural Network (NN) has two components. The first is a CNN that takes as input real-scale images of the beam cross-sections used for training. The CNN, which works as a feature extractor, uses Sobel and Laplace filters to extract valuable geometric information from the images. For each structural case, the CNN output vector is concatenated with a vector containing the specific structural theory used, the slenderness ratio (L/h), and the beam material. Each structural theory is encoded as a sequence of 0s and 1s, where 1 represents an active generalized variable, e.g.,

$$u_x = u_{x_1} + xu_{x_2} + x^2u_{x_4} + z^2u_{x_6} = [1\ 1\ 0\ 1\ 0\ 1] \quad (6)$$

The resulting arrays are fed into a DNN trained on the average error of the first 10 natural frequencies with respect to the reference fourth-order theory for each structural case computed by AAM. The trained NN predicts the accuracy of a kinematic theory for a generic structural case, taking as inputs the image of the cross-section, the L/h ratio, and the beam material, see Fig. 2.

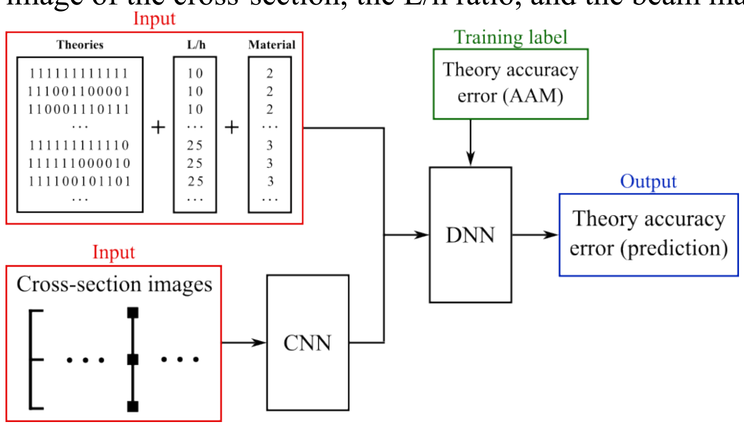

Figure 2: NN architecture

Numerical Results

The dataset consists of 1080 structural cases, each computed using AAM. Each AAM analysis comprises 4096 FEM modal analyses. To train the DNN, only 10% of these analyses were randomly selected and used. The results shown hereafter refer to two different beams, both clamped-free and made of titanium. The material properties are: E=115 GPa, ν=0.33, ρ=4500 kg/m^3. The first, whose cross-section is shown in Fig. 3, is a stiffened spar included in the network training. The length L is equal to 10m, the height of the cross section is 1m, the sides of the three equally spaced squared stiffeners are 4 cm, while the thickness of the web is 2 mm. The Best Theory Diagrams (BTD) computed by AAM and DNN are shown in Fig. 4, while Tables 1 and 2 report the best theories and their accuracies, from AAM and DNN, respectively. In these tables, the black triangle indicates that the generalized variable is active. The network's predictive capabilities were analyzed by testing different beams not used during network training. A stiffened spar not involved in the network training is shown in Fig. 5, with a length L of 8 m, a height "h" of the cross-section of 1 m, and the side of the squared stringer is 4 cm. The web thickness is 2 mm. The stringers are not equally spaced, with the middle stringer located at h/3 from the bottom of the cross-section. Figure 6 shows the BTD for this structural case, while Tables 3 and 4 report the best theories and their accuracies.

Figure 3: Stiffened spar cross-section included in the network training

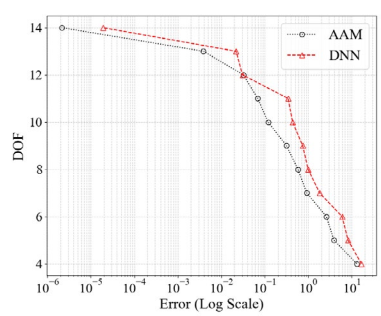

Figure 4: BTD of the stiffened spar included in the network training

DOF	const.	x	z	x^2	xz	z^2	x^3	x^2z	xz^2	z^3	x^4	x^3z	x^2z^2	xz^3	z^4	$\%E_{AVG}$
14	▲	▲	▲	▲	▲	▲	▲	▲	▲	▲	△	▲	▲	▲	▲	2.141E-06
13	▲	▲	▲	▲	▲	▲	△	▲	▲	▲	△	▲	▲	▲	▲	3.877E-03
12	▲	▲	▲	▲	▲	▲	△	▲	▲	▲	△	▲	△	▲	▲	3.216E-02
11	▲	▲	▲	▲	▲	▲	△	▲	▲	△	△	▲	△	▲	▲	6.892E-02
10	▲	▲	▲	▲	▲	▲	△	▲	▲	△	△	△	△	▲	▲	1.193E-01
9	▲	▲	▲	▲	▲	▲	△	▲	▲	△	△	△	△	▲	△	3.167E-01
8	▲	▲	▲	▲	▲	▲	△	△	▲	△	△	△	△	▲	△	5.798E-01
7	▲	▲	▲	▲	▲	▲	△	△	▲	△	△	△	△	△	△	9.229E-01
6	▲	▲	▲	▲	▲	▲	△	△	△	△	△	△	△	△	△	2.604E+00
5	▲	▲	▲	▲	▲	△	△	△	△	△	△	△	△	△	△	3.903E+00
4	▲	▲	▲	△	▲	△	△	△	△	△	△	△	△	△	△	1.305E+01

Table 1: Best theories from AAM of the stiffened spar included in the network training

DOF	const.	x	z	x^2	xz	z^2	x^3	x^2z	xz^2	z^3	x^4	x^3z	x^2z^2	xz^3	z^4	$\%E_{AVG}$
14	▲	▲	▲	▲	▲	▲	▲	▲	▲	▲	△	▲	▲	▲	▲	1.897E-05
13	▲	▲	▲	▲	▲	▲	△	▲	▲	▲	△	▲	▲	▲	▲	2.193E-02
12	▲	▲	▲	▲	▲	▲	△	▲	▲	▲	△	▲	△	▲	▲	3.064E-02
11	▲	▲	▲	▲	▲	▲	△	▲	▲	▲	△	△	△	▲	▲	3.443E-01
10	▲	▲	▲	▲	▲	▲	△	▲	▲	△	△	△	△	▲	▲	4.374E-01
9	▲	▲	▲	▲	▲	▲	△	△	▲	▲	△	△	△	▲	△	7.439E-01
8	▲	▲	▲	▲	▲	▲	△	△	▲	△	△	△	△	▲	△	9.949E-01
7	▲	▲	▲	▲	▲	▲	△	△	▲	△	△	△	△	△	△	1.820E+00
6	▲	▲	▲	▲	▲	▲	△	△	△	△	△	△	△	△	△	6.002E+00
5	▲	▲	▲	▲	▲	△	△	△	△	△	△	△	△	△	△	8.217E+00
4	▲	▲	▲	△	▲	△	△	△	△	△	△	△	△	△	△	1.665E+01

Table 2: Best theories from DNN of the stiffened spar included in the network training

Figure 5: Stiffened spar cross-section not included in the network training

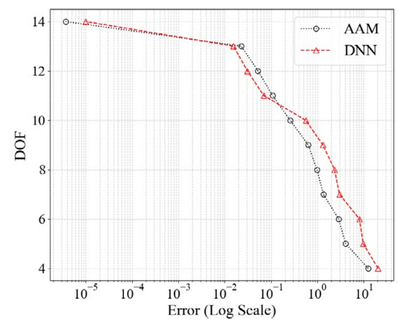

Figure 6: BTD of the stiffened spar not included in the network training

DOF	const.	x	z	x^2	xz	z^2	x^3	x^2z	xz^2	z^3	x^4	x^3z	x^2z^2	xz^3	z^4	$\%E_{AVG}$
14	▲	▲	▲	▲	▲	▲	▲	▲	▲	▲	△	▲	▲	▲	▲	3.664E-06
13	▲	▲	▲	▲	▲	▲	△	▲	▲	▲	△	▲	▲	▲	▲	2.275E-02
12	▲	▲	▲	▲	▲	▲	△	▲	▲	▲	△	△	▲	▲	▲	5.252E-02
11	▲	▲	▲	▲	▲	▲	△	▲	▲	▲	△	△	△	▲	▲	1.078E-01
10	▲	▲	▲	▲	▲	▲	△	▲	▲	△	△	△	△	▲	▲	2.586E-01
9	▲	▲	▲	▲	▲	▲	△	△	▲	△	△	△	△	▲	▲	6.384E-01
8	▲	▲	▲	▲	▲	▲	△	▲	▲	△	△	△	△	△	△	9.796E-01
7	▲	▲	▲	▲	▲	▲	△	△	▲	△	△	△	△	△	△	1.354E+00
6	▲	▲	▲	▲	▲	▲	△	△	△	△	△	△	△	△	△	2.882E+00
5	▲	▲	▲	▲	▲	△	△	△	△	△	△	△	△	△	△	4.086E+00
4	▲	▲	▲	△	▲	△	△	△	△	△	△	△	△	△	△	1.254E+01

Table 3: Best theories from AAM of the stiffened spar not included in the network training

DOF	const.	x	z	x^2	xz	z^2	x^3	x^2z	xz^2	z^3	x^4	x^3z	x^2z^2	xz^3	z^4	$\%E_{AVG}$
14	▲	▲	▲	▲	▲	▲	▲	▲	▲	▲	△	▲	▲	▲	▲	9.893E-06
13	▲	▲	▲	▲	▲	▲	△	▲	▲	▲	△	▲	▲	▲	▲	1.547E-02
12	▲	▲	▲	▲	▲	▲	△	▲	▲	▲	△	▲	△	▲	▲	3.097E-02
11	▲	▲	▲	▲	▲	▲	△	▲	▲	▲	△	△	△	▲	▲	6.975E-02
10	▲	▲	▲	▲	▲	▲	△	△	▲	▲	△	△	△	▲	▲	5.599E-01
9	▲	▲	▲	▲	▲	▲	△	△	▲	▲	△	△	△	▲	△	1.320E+00
8	▲	▲	▲	▲	▲	▲	△	△	▲	△	△	△	△	▲	△	2.359E+00
7	▲	▲	▲	▲	▲	▲	△	△	▲	△	△	△	△	△	△	3.007E+00
6	▲	▲	▲	▲	▲	△	△	▲	△	△	△	△	△	△	△	8.118E+00
5	▲	▲	▲	▲	▲	△	△	△	△	△	△	△	△	△	△	9.807E+00
4	▲	▲	▲	△	▲	△	△	△	△	△	△	△	△	△	△	2.041E+01

Table 4: Best theories from DNN of the stiffened spar not included in the network training

Conclusion

This work presents a methodology and a tool for the accuracy estimation of a beam theory and its generalized variables for a given problem. In addition, it assesses the minimum number of DOF required to obtain that level of accuracy. The proposed methodology uses NN to correlate structural theories, geometries, materials, and accuracy. The results show a strong correlation between AAM results and DNN predictions for the beams included in the network's training set. For those not included in the training, the results remain excellent for accuracy prediction, while the correlation slightly decreases for predicting the best theories. The results indicate that, in both cases, achieving errors below 10% requires at least two parabolic terms, while errors under 1% can only be ensured by using the complete parabolic expansion along with two or three additional higher-order terms. The results are highly problem-dependent, as the specific higher-order terms involved vary from case to case.

References

[1] Euler L. De curvis elasticis. Lausanne and Geneva: Bousquet, 1744.

[2] Timoshenko S.P. On the transverse vibrations of bars of uniform cross-section. The London, Edinburgh, and Dublin Philosophical Magazine and Journal of Science, 43(253):125-131, 1922. https://doi.org/10.1080/14786442208633855

[3] Timoshenko S.P. On the correction for shear of the differential equation for transverse vibrations of prismatic bars. The London, Edinburgh, and Dublin Philosophical Magazine and Journal of Science, 41(245):744-746, 1921. https://doi.org/10.1080/14786442108636264

[4] Carrera E. and Petrolo M. On the effectiveness of higher-order terms in refined beam theories. Journal of Applied Mechanics, 78(2):021013, 11 2010. https://doi.org/10.1115/1.4002207

[5] Carrera E., Pagani A., Petrolo M., and Zappino E. Recent developments on refined theories for beams with applications. Mechanical Engineering Reviews, 2(2):14-00298-14-00298, 2015. https://doi.org/10.1299/mer.14-00298

[6] Giunta G., Biscani F., Belouettar S, Ferreira A.J.M., and Carrera E. Free vibration analysis of composite beams via refined theories. Composites Part B: Engineering, 44(1):540-552, 2013. https://doi.org/10.1016/j.compositesb.2012.03.005

[7] Petrolito J. Stiffness analysis of beams using a higher-order theory. Computers & Structures, 55(1):33-39, 1995. https://doi.org/10.1016/0045-7949(94)00505-W

[8] Argyridi A.K. and Sapountzakis E.J. Higher order beam theory for linear local buckling analysis. Engineering Structures, 177:770-784, 2018. https://doi.org/10.1016/j.engstruct.2018.08.069

[9] Carrera E., Cinefra M., Petrolo M., and Zappino E. Finite element analysis of structures through unified formulation. John Wiley & Sons, 2014. https://doi.org/10.1002/9781118536643

[10] Petrolo M., Iannotti, P. Best Theory Diagrams for Laminated Composite Shells Based on Failure Indexes. Aerotec. Missili Spaz. 102, 199-218 (2023). https://doi.org/10.1007/s42496-023-00158-5 https://doi.org/10.1007/s42496-023-00158-5

[11] Thai H.-T., Machine learning for structural engineering: A state-of-the-art review. Structures, 38:448-491, 2022. https://doi.org/10.1016/j.istruc.2022.02.003

[12] Petrolo M., Pagani A., Carrera E., Candita G., Iannotti P. Mapping beam cross-section features to higher-order generalized variables using machine learning. Thin-Walled Structures, Volume 218, Part C, (2026). https://doi.org/10.1016/j.tws.2025.114108 https://doi.org/10.1016/j.tws.2025.114108

[13] Petrolo M., Pagani A., Candita G., Iannotti P., and Carrera E. Assessment of multi-fidelity structural theories for dynamic analyses using machine learning. In Proceedings of the ASME 2025 Aerospace Structures, Structural Dynamics, and Materials Conference SSDM2025, Houston, 2025. https://doi.org/10.1115/SSDM2025-152306